RESEARCH ARTICLE

European Journal of Advanced Chemistry Research
www.ej-chem.org

Synthesis and Characterization of Antibacterial Photocatalytic Activated Carbon Black-Titanium Dioxide Composite Employing Ultrasonic Agitation Method

Mega Fatimah and Pratama Jujur Wibawa

ABSTRACT

The functional composites of activated carbon black-titanium dioxide (ACB-TiO_2) with antibacterial-photocatalytic properties have been properly synthesized in this research using ultrasonic of 40 kHz, 2×50 W at 50 ºC for 10, 20, and 30 minutes agitation time. This research aimed to enhance titanium dioxide's antibacterial and photocatalytic properties (TiO_2) using activated carbon black (ACB) particles forming ACB-TiO_2 composites. The antibacterial properties of the materials were evaluated based on their capability of inhibiting Escherichia coli (gram-negative) and Staphylococcus aureus (gram-positive) bacteria cells growth, while the photocatalytic properties of them were evaluated based on their capability of degrading methyl orange dye molecules under ultraviolet (UV) light exposure. It is conclusively known that the ACB-TiO_2 composites can be synthesized from the activated carbon black (ACB) and titanium dioxide (TiO_2) of about 164 nm and 547 nm in their particle size respectively employed ultrasonic agitations for the various time. All of the produced ACB-TiO_2 composites could inhibit the bacterial cell growth and also could decompose the methyl orange molecules with the best was that synthesized using 30 minutes ultrasonic agitation time.

Keywords: Activated Carbon Black, Antibacterial Properties, Composites, Photocatalysis, Titanium Dioxide.

Published Online: May 11, 2023

ISSN: 2684-4478

DOI: 10.24018/ejchem.2023.4.3.133

M. Fatimah
The National Research and Innovation Board of Indonesia (BRIN), Indonesia
(e-mail: mega013@brin.go.id)
P. J. Wibawa *
Organic Chemistry Laboratory Department of Chemistry, Faculty of Sciences and Mathematics, Diponegoro University, Indonesia
(e-mail: pratamajw@live.undip.ac.id)

**Corresponding Author*

I. Introduction

Since the last decade, composite materials have a great deal of attention due to the ease of fabricating to fulfill the requirements of various usages and applications. It is because composites are synthetic materials constructed by two or more materials constituents of different properties each other where overall forming a new single property and the properties of the constituents still exist in it [1]. Thus, the properties of composites can be well determined from early when someone would like to synthesize the composites by means of choosing the starting materials that have suitable properties to fulfill the requirements of applications who wanted. In this case, one of the constituents of the major quantity takes a role as a matrix of the associated composites and the others as fillers or binders. Nevertheless, it is also possible that a composite can be constructed by eliminating the matrix if nothing is a majority in the number of its constituents. For instance, [2] used ethyl vinyl acetate (EVA) as a matrix and dimethyl dialkyl (C14-C18) amine as an organic surfactant for nanofiller in the fabrication of EVA-based composite for biomedical applications due to EVA having high biocompatibility and biostability properties while dimethyl dialkyl (C14-C18) amine has the capability of tremendous improvement of the physical and mechanical properties of the synthesized composite. [3] used TiO_2 and MoS_2 to synthesize MoS_2/TiO_2–based nanocomposites for application in photocatalysis and rechargeable batteries due to TiO_2 has strong optical absorption, which is promising for photocatalysis, while MoS_2 has high catalytic activity. Another research team, [4] used polyvinyl alcohol (PVA) and multiwall carbon nanotubes (MWCNT) as raw materials to synthesize a PVA/MWCNT composite that has the capability of simultaneous removal of methyl red dye and heavy metals from industrial wastewater effluent due to PVA can form a hydrogen bond with the dye while MWCNT adsorbs heavy metals on its cylindrical hollow structure.

In relation to producing advanced and smart materials to supply the materials demands in the 4th industrial revolution era today so composite materials technology is the most possible way for that. In the field of human health and environmental safety, for example, titanium dioxide (TiO_2) has been widely recognized as an effective agent to photo catalytically degrade any toxic organic pollutants spreading in a ubiquitous

European Journal of Advanced Chemistry Research
www.ej-chem.org

area of human life [5]-[9] as well as to protect human from the pathogenic microorganisms' contaminations including bacteria, viruses, and fungi [10], [11]. The energy band gap inherently reveals between the valence band (VB) and conduction band (CB) of TiO_2 anatase of about 3.0-3.2 eV [7], [12] facilitates electrons to jump from the VB to CB when the ultraviolet-visible (UV-Vis) light hit it. The jumping of electrons leaves reactive holes in VB that enable to acceptance of electrons coming from hazardous pollutants as well as from compounds constructed in the bacteria cell wall, fungi, and viruses so that they all will be decomposed and die.

Another possibility, the jumped electrons readily induce the generation of reactive oxygen species (ROS) such as hydroxyl radical, super acid, or hydroperoxide radical depending on the medium (solvent and matrix) used. Several researchers proved that the generated ROS is a very important molecular key in causing bacteria, viruses, and fungi death, and organic pollutants decomposition [12]-[15]. These facts lead to TiO_2 being a more advantageous chemical for the synthesis of TiO_2 −based antimicrobial material or as a super active agent for an alternative antibiotic drug replacing organic molecules-based antibiotics in which many pathogenic microbes have been resistant.

In addition, the pores of the activated carbon black would be able to adsorb the bacterial cells, especially the pores bigger than the bacterial cells in its size. If the activated carbon black pores could be properly enriched with TiO_2 particles, the absorbed bacteria would be killed faster. It is because not only were nothing bacteria nutrients present inside the pores but also the bacteria were hit by the ROS particles. Accordingly, the synthesized composite of the activated carbon black and TiO_2 particles would have become a very effective photo-catalytically antibacterial material.

Currently, many TiO_2–based composites with not only possessed antimicrobials activity but also belong to photocatalytic and anticancer activity have been successfully synthesized by using various counterpart matrices such as ZnO [16], Epoxy resin polymer [17], Polycaprolactone matrix [18], AgCl and Folic acid [19], SiO_2 and ZrO_2 [20] and so on. In these all cases, the role of the counterpart materials was to enhance the chemical and physical properties of TiO_2 including its antibacterial and photocatalytic activity by decreasing its energy band gap reveal between VB and CB so that the electromagnetic visible light spectrum can force the VB electrons to jump into the CB surface. However, the effect of the parous material properties for the enhancement of the photocatalytic antimicrobial properties of the synthesized TiO_2-based composite has not been investigated at all yet in such composite synthesis. Therefore, this paper reports the effect of highly porous material represented by activated carbon black particles in enhancing the antibacterial properties of TiO_2 in the form of activated carbon black-TiO_2 composite (ACB-TiO_2). In addition, the effect of the ultrasonic agitation times for the enhancement of the antibacterial properties of the fabricated ACB-TiO_2 composite was also studied in this research.

II. Experimental Section

A. Materials

Local available commercial carbon black powder, Tween 20, Distilled water, Double distilled water, Phosphoric acid (H_3PO_4), Titanium (IV) chloride ($TiCl_4$), locally available Aloe vera extract, Filter paper Whatman No.42, Amoxicillin, Agarose, Yeast extract, Ethyl alcohol (C_2H_6O) 70%, Bacto peptone, Methyl orange. All the chemicals mentioned are in pure analysis grade and produced in Germany.

B. Instruments

Laboratory glass wares, Ball milling machine, Electrical furnace, Electrical oven, pH meter, Ultrasonic cleaner (40 kHz 2 × 50 W, Krisbow, China), Autoclave, Incubator, Laminar air flow box, Scanning electron microscope-Energy dispersive X-ray (SEM-EDX) spectroscopy (JEOL JSM-6510 LA Japan), Particles size analyzer (PSA) (Horiba SZ-100, USA), Ultraviolet-Visible (UV-Vis) spectrophotometer (Shimadzu Corp. Japan model UV-1280, Japan), Ultraviolet (UV) blacklight reactor 365 nm wavelength, 10 W (Sankyo Denki, Japan), X-ray dispersion (XRD) spectroscopy (Shimadzu XRD 7000s, Japan), Fourier Transform Infrared (FTIR, Perkin Elmer V.10.400, USA).

The research performed started with the fabrication of activated carbon black (ACB) particles and was subsequently followed by the fabrication of TiO_2 microparticles (TiO_2MPs), the determination of particles size distribution of the fabricated ACB and TiO_2 microparticles using a PSA machine based on the dynamic light scattering (DLS) method, the synthesis of ACB-TiO_2 composite, the photo catalytically antibacterial activity test, and finally the surface morphology analysis of the fabricated ACB-TiO_2 using SEM-EDX spectroscopy. The comprehensive research work was then described in the subsections below in detail.

C. Fabrication of ACB Microparticles

The local commercially available carbon black powder of about 100 grams was crushed further up to it and passed through a 200 meshes sieve in size using a ball milling machine. Three samples of every 0.25

gram the carbon black fine powder produced each encoded as ACB1, ACB2, and ACB3 then independently mixed properly with 2 drops Tween 20, 0.25 gr H_3PO_4, and 200 mL distilled water as performed by [21] with a little bit modification. This mixture was stirred continuously in a magnetic stirrer bar for one hour to make it surely becomes homogeneous and kept it on a room temperature for overnight (24 hours) standby. Furthermore, the mixture was treated with ultrasonic wave (40 kHz, 2 × 50 W) for various times of 30, 60 dan 90 minutes each for ACB1, ACB2, and ACB3 samples codes, respectively. It is very important that the three samples aforementioned are to have a pH of about 7 (pH neutral) so the samples were then washed up with distilled water several times until pH neutral reached. Finally, the samples were heated at 250°C for 6 hours in an electrical oven to remove the water medium and then followed thermal activation at 500°C for 1 hour in a furnace. The products are the desired activated carbon black microparticles of ACB1, ACB2, and ACB3 quality grades due to the ultrasonic effect ready for further analysis, characterization, and use.

D. Synthesis of TiO_2 microparticles (TiO_2MPs)

TiO_2MPs were synthesized greenly from its precursor, i.e., $TiCl_4$ using freshly prepared water-Aloe vera extract according to [22] procedure with a little bit of modification. It was performed as follows in detail, the Aloe vera extract of about 100 mL volume was added into 10 mL $TiCl_4$ 1.0 N under a continuous stirrer for 1 hour then let on a room temperature for about 24 hours overnight. At this moment the desired TiO_2MPs would have been sedimented on the bottom of the flask and it was then separated from its aqueous medium using Whatman No.42 filter paper and washed up three times with distilled water to remove the impurities generated during the fabrication process. After that, the fabricated TiO_2MPs were dried using an electrical oven at 100°C for 1 hour and calcinated at 500°C for 4 hours. Finally, the particle size and crystallinity of the fabricated TiO_2MPs were further analyzed by using PSA and XRD respectively.

E. Synthesis of ACB-TiO_2 Composite

The ACB-TiO_2 composite was synthesized by mean of incorporating the fabricated TiO_2MPs onto the fabricated ACB microparticles with a 1:1 weight ratio in 5 mL double distilled water under ultrasonic treatment for various times of 10, 20 dan 30 minutes after the mixture had already been stirred with a magnetic stirrer bar at 50°C for 1 hour. Furthermore, the composite obtained was dried up in an electrical oven in which the temperature was set up at 100°C for 1 hour, and finally, it was heated at 500°C for 4 hours using an electrical furnace.

F. Antibacterial Activity Test of ACB-TiO_2 Composite

The photocatalytic antibacterial activity test of the synthesized ACB-TiO_2 composite was confirmed towards both Escherichia coli and Staphylococcus aureus bacterial cell cultures by an agarose disc diffusion method. Under this method, the bacteria were first activated independently in a liquid medium freshly made of 0.25-gr peptone and 0.05-gram yeast at about 37°C temperature for 24 hours of incubation. After that, the active bacterial cultures were grown up on the solid medium freshly made of 0.1875-gr peptone, 0.0375-gr yeast, and 1.125-gr agarose in which five Whatman filter paper discs of around 1 cm in diameter of which the first disc wetted by the aqueous colloidal ACB-TiO_2 composite, the second disc by amoxicillin antibiotic solution (positive control), the third just by distilled water (negative control), the fourth by aqueous colloidal ACB microparticles (comparison material I), and the fifth by aqueous colloidal TiO_2 microparticles (comparison material II) had been properly embedded on the surface of the medium. A clear zone around the Whatman filter paper disc after 24 hours of incubation at 37°C temperature under UV light exposure and under visible light exposure indicated that the associated sample has antibacterial activity. The wider the clear zone generation means the better the antibacterial activity.

G. Photocatalytic Activity Test of ACB-TiO_2 Composite

The photocatalytic activity test of the synthesized ACB-TiO_2 composite was performed by mean of mixing 0.1 gram of the composite and 50 mL methyl orange (MO) solution of 100 mg/L (ppm) concentration for 1 hour long under UV light exposure as well as under visible light exposure. The composite was then separated from the MO solution by filtration method employing Whatman filter paper No. 42 followed the time for the adsorption capability test was over. The amount of remaining MO was then determined by using UV-Vis spectrophotometer at 465 nm wavelength. The UV-Vis absorbance value of the MO solution was then converted to ppm by applying a standard curve of MO solution correlated UV-Vis absorbance value at 465 nm wavelength versus its concentration in ppm unit, which was already prepared first. The photocatalytic capability of the ACB-TiO_2 composite was evaluated by applying (1), (2), and (3).

In (1), (2), and (3), MOd_{vis} is degraded MO under visible light exposure; MOd_{uv} is degraded MO under UV light exposure; Cf_{vis} is the final MO concentration in ppm unit after photocatalytic test under visible light exposure; Ci_{vis} is initial MO concentration in ppm unit before photocatalytic test under visible light exposure; Cf_{uv} is final MO concentration in ppm unit after photocatalytic test under UV light exposure, Ci_{uv}

is initial MO concentration in ppm unit before photocatalytic test under UV light exposure and P_{cab} is the photocatalytic capability of the tested composite. Here, the bigger the P_{cab} means the better the photocatalytic capability of the associated composite.

$$\%MOd_{vis} = [(Ci_{vis} - Cf_{vis} \div Ci_{vis}] \times 100\% \quad (1)$$

$$\%MOd_{uv} = [(Ci_{uv} - Cf_{uv} \div Ci_{uv}] \times 100\% \quad (2)$$

$$P_{cab} = [(\%MOr_{uv} - \%MOr_{vis}) \div \%MOr_{vis}] \times 100\% \quad (3)$$

H. Analysis and Characterization of the ACB-TiO_2 Composite

The surface morphology of the synthesized ACB-TiO_2 composite and the distribution of TiO_2 on the associated ACB surface was confirmed by using SEM-EDX spectroscopy run with elementary mapping mode.

III. Results and Discussion

A. Fabrication of ACB Microparticles

The particle size distribution of ACB microparticles produced in this research was statistically displayed in Fig. 1. Fig. 1 shows that 30, 60, and 90 minutes of ultrasonic agitation could produce the ACB microparticles that presented as Z-average in size of 139.5, 178.9, and 175.8 nm, respectively. The polydispersity index (PI) of the particles that is the parameter of uniformity of the particle sizes is also shown in Fig. 1; *i.e.*, 0.172, 0.318, and 0.354 each for 30, 60, and 90 minutes of ultrasonic agitation respectively. In association with the typical curve of the particle sizes distribution, we can see that 30-minute ultrasonic provides more narrow sizes and is subject to the normal distribution curve model compared to 60 minutes as well as 90 minutes of ultrasonic agitation. These data demonstrated that more uniform sizes of the ACB particles provide smaller PI in value. In addition, the PSA software inherently installed in the associated instrument also released the statistical calculation results expressed as mean value, standard deviation (SD) value, and mode value of the particle sizes distribution. The original data of those are collected as an additional appendix of the reference [23] of this paper.

It was well known that the mean, SD, and mode of the sizes of the ACB particles were about 164.3 nm, 67.6 nm, and 142.5 nm respectively all produced for 30 minutes of ultrasonic agitation. It means that the sizes of 50% population of the ACB microparticles be less than 164.3 nm and the other 50% population of that be more than 164,3 nm. Furthermore, based upon the SD value it was exactly known the size range of the throughout ACB microparticles be 164.3 ± 67.6 nm, or in other words the sizes of the smallest particles were about 96.7 nm and the biggest ones about 231.9 nm. Among them, the particle sizes of 142.5 nm were the most frequently recorded by the PSA detector as indicated by the mode value of the particle size 142.5 nm.

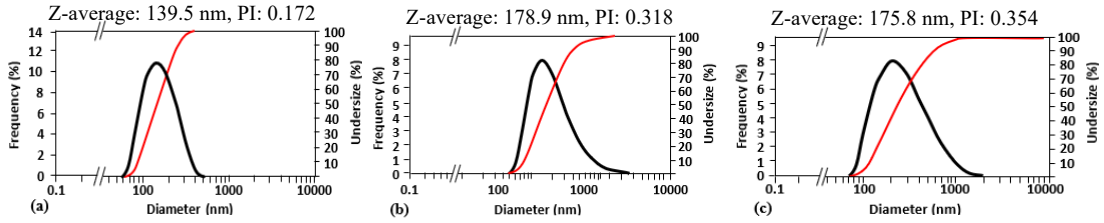

Fig. 1. The particle sizes distribution of ACB microparticles produced through ultrasonic agitation for: (a) 30 minutes, (b) 60 minutes, and 90 minutes [23].

On the other hand, the values of mean, SD, and mode of the sizes of the ACB microparticles produced by 60 minutes of ultrasonic agitation were 225.1 nm, 183.8 nm, and 126.5 nm respectively. By a similar interpretation as above, we know that the sizes range of the ACB microparticles mentioned varies from the smallest, 41.3 nm up to the biggest ones, 408.9 nm so that it can be written as 225.1 ± 183 nm. This size range is very large compared to that of producing by 30 ultrasonic agitations, attributed that the associated ACB microparticles are not so uniform in size. A similar result was also shown by the ACB microparticles produced through 90 minutes of ultrasonic agitation. In this case mean value, SD, and mode values of the sizes of the ACB microparticles produced by 90 minutes of ultrasonic agitation were 287.8 nm, 191.4 nm, and 182.4 nm respectively. It demonstrated the size range of the associated ACB microparticles was more varied in size starting from 96.4 nm up to 479.2 nm so that it can be written as 287.8 ± 191.4 nm.

The most interesting of the experimental data aforementioned is the smaller size of the ACB microparticles namely nano-scale sizes are precisely produced by the shorter time of ultrasonic agitation, 30 minutes instead of the longer one, 60 and 90 minutes. Accordingly, we can focus our attention just on 30 minutes of ultrasonic agitation time rather than the others; it is, in particular, to produce nanoscale ACB microparticles in size. Of course, using short times of ultrasonic agitation in producing ACB microparticles has many advantages such as less time and energy consumption, and avoiding the agglomeration process going on continuously. It is because the agglomeration process may happen throughout ACB microparticles exposed to ultrasonic for more than 30 minutes. Furthermore, the synthesized ACB microparticles by 30 minutes of ultrasonic agitation were preferred to be used as a matrix for the desired composite synthesis.

B. Synthesis of TiO_2 Microparticles

The result of the synthesis of TiO_2 microparticles from $TiCl_4$ precursors employing aqueous-Aloe vera extract was visually depicted in Fig. 2. In this case, we prefer focusing our attention on Fig. 2c in which the chemical reactions transforming Ti^{+4} ions gradually became Ti metal microparticles (TiO_2MPs) clearly occurred since the brown color deposit was generated.

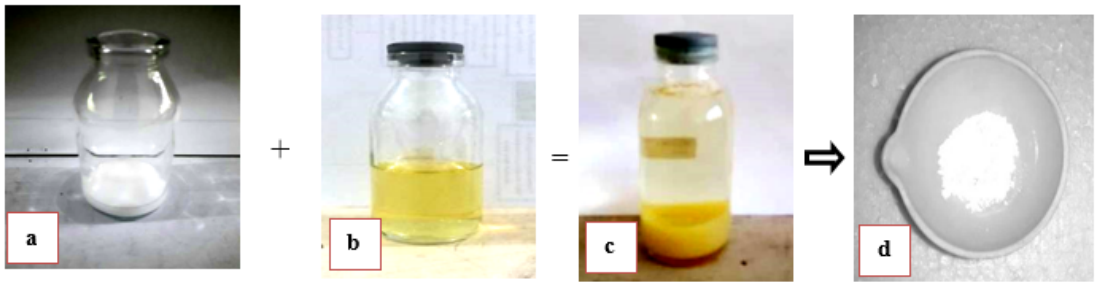

Fig. 2. The photograph of color change in the synthesis of TiO2MPs starting from (a) TiCl4 solution as Ti precursor of white color suspension, (b) aqueous Aloe vera extract of bright-yellow color, (c) The mixture of TiCl4 solution and aqueous Aloe vera extract, the brown color deposit was formed, (d) White color powder of the desired TiO2MPs produced [23].

In this context, several secondary metabolite natural products of the aqueous Aloe vera extract such as flavonoid, saponin, and tannin [24] simultaneously took a role as reducing agents by delivering their lone pair electrons of the polyhydroxy group atomic oxygen to the Ti^{+4} ions so that it became Ti metal atoms. This situation might just happen at a few seconds so that the associated Ti atom immediately oxidized again by gaining oxygen atoms that came from the associated aqueous medium as aqueous-soluble reactive oxygen species (ROS') to be TiO_2 molecules due to the standard oxidation potential of Ti atom is high enough. However, in this context, [25] have successfully investigated through a thermochemistry approach instead of electrochemistry and proved that TiO_2 could be properly formed from $TiCl_4$ precursor by hydrolysis process through the formation of several intermediates, titanium oxychloride acid such as TiOClOH and $TiCl_2(OH)_2$. Furthermore, the TiOClOH and $TiCl_2(OH)_2$ could spontaneously release hydrochloric acid (HCl) molecule(s) to become TiO_2 according to (4) and (5) respectively [25].

$$TiOClOH \rightarrow TiO_2 + HCl + Q_1 \text{ kcal} \quad (4)$$

$$TiCl_2(OH)_2 \rightarrow TiO_2 + 2HCl + Q_2 \text{ kcal} \quad (5)$$

These TiO_2 molecules have a high capability of interface interaction with each other due to their high surface area to volume ratio through van der Waals driving force mechanism. Subsequently, the TiO_2 molecules undergo a limited agglomeration process during ultrasonic agitation to be TiO_2 microparticles in various sizes. In this relation, flavonoid, saponin, and tannin composing the Aloe vera extract simultaneously covered the formed TiO_2 microparticles and act as suitable stabilizer agents specifically through hydrogen bonding interactions as reported by [26]. Owing to this the sizes of TiO_2 microparticles were properly determined by the molecules' amount of flavonoid, saponin, and tannin that directly covered them through the hydrogen bonding. This situation can force the TiO_2 microparticles experiencing re-self-assembly to be spherical shape particles micro-structured and also similar to the core-shell microstructure materials. The core-shell microstructure of TiO_2 microparticles forming the spherical shape microparticles representative is hypothetically proposed as depicted in Fig. 3.

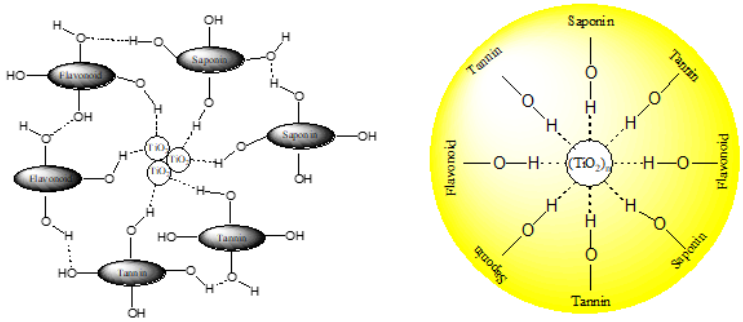

Fig. 3. Hypothetically model of the formation of core-shell spherical shape structure of Aloe vera extract-stabilized TiO_2 microparticle, (a) Agglomerated TiO_2 molecules stabilized by hydrogen bonds of the Aloe vera extract components, flavonoids, saponins, and tannins, (b) The size of the TiO_2 microparticles counted by PSA instrument. Here, the dashed lines are representing hydrogen bonds.

In correlation to the sizes of the synthesized TiO_2 microparticles, it has been properly confirmed by the DLS method using a PSA instrument and obtained about 388.3 nm with a PI of 0.617. While the statistical curve expressing the size distribution of the TiO_2 microparticles in detail is depicted in Fig. 4.

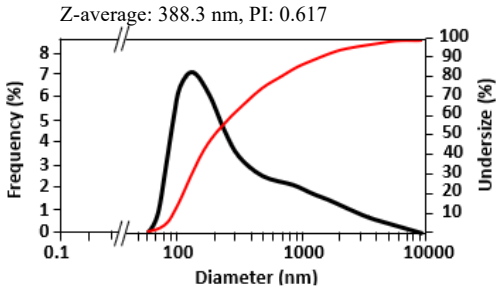

Fig. 4. Statistical curve of the synthesized TiO2 microparticles distribution [23].

Fig. 4 shows a non-normal curve representing the very low uniformity of the TiO_2 microparticles produced and indicated the size range of the particles is very large. It is matched with the statistical calculations that provided the value of the mean, SD, and mode sizes of the synthesized TiO_2 microparticles were about 547.7 nm, 948.4 nm, and 126.0 nm respectively. The original data of those are collected as an additional appendix of the reference [23] of this paper.

Furthermore, surface morphology images and the analysis of trace element compositions of the synthesized TiO_2 microparticles explored with SEM-EDX spectrometer are displayed in Fig. 5.

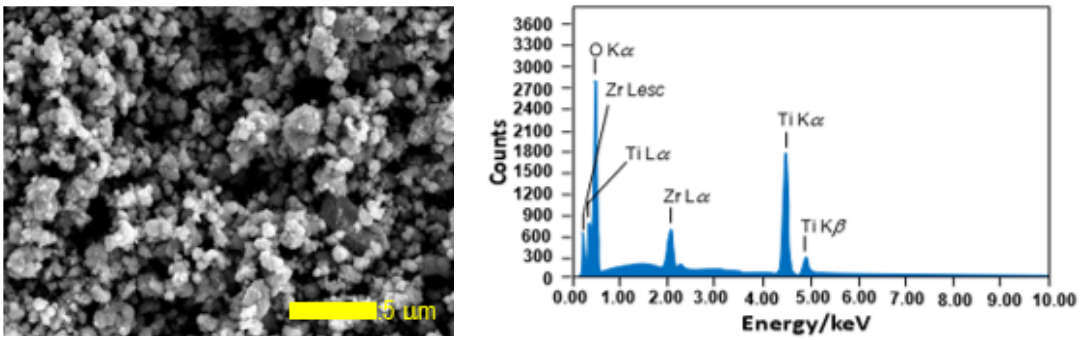

(a) (b)

Fig. 5. (a) The SEM image of the synthesized TiO_2 microparticles, 5000× magnification, (b) The EDX spectrogram of the associated TiO_2 microparticles [23].

Fig. 5 shows agglomerated spherical shape structure of the synthesized Aloe vera extract–stabilized TiO_2 microparticles of about 300-500 nm in size. This result matches the hypothetical structure proposed shown in Fig. 3 and is similar to TiO_2 obtained by [27]. While that, the EDX analysis result of the synthesized TiO_2 microparticles displayed in Fig. 3b confirmed that several elements not only Titanium (Ti) but also Carbon (C), Oxygen (O), and Zirconium (Zr) present in these particles with different concentration of 49.64%, 5.29%, 37.20% and 7.94% respectively. The original data of those are collected as an additional appendix of the reference [23] of this paper.

This data precisely justifies and can be evident that the Aloe vera extract components have properly covered the synthesized TiO_2 micro particles due to the oxygen and carbon elements coming from the polyhydroxy groups of flavonoids, saponin, and tannin, while another element, *i.e*. Zr is impurities brought by the Aloe vera extract.

C. Synthesis of ACB-TiO₂ Composite

Visually, grey-black color particles of ACB-TiO_2 composite were successfully synthesized in this research by various times ultrasonic agitation of 10, 20, and 30 minutes. However, the deposit of the ACB-TiO_2 composite was not generated during 30 minutes of ultrasonic agitation including when it was left at room temperature for 24 hours or overnight. It demonstrated that the ACB-TiO_2 composite synthesized through 30 minutes of ultrasonic agitation was the most stable product of the associated composites in a water-oil dispersion system. This case indicated that TiO_2 microparticles have successfully entered into the pores of the ACB supporting material and are properly distributed throughout the surface of it due to the ultrasonic agitation. Referring to [28], it can be understood that the applied ultrasonic wave hit the throughout materials present in the associated mixture and vibrate vigorously, including opening the ACB pores so that TiO_2 molecules entered and settle down in the associated pores.

The surface morphology and TiO_2 molecules distribution mapping of the synthesized ACB-TiO_2 composite explored with SEM-EDX spectrometer are displayed in Fig. 6.

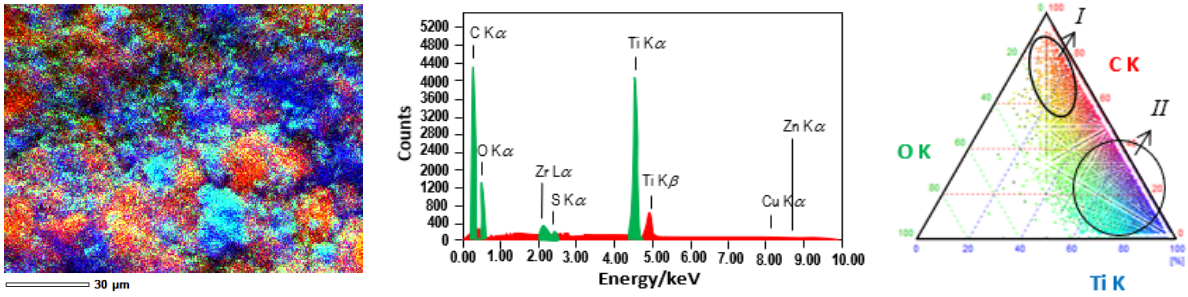

(a) (b) (c)

Fig. 6. (a) SEM-EDX images of the synthesized ABC-TiO_2 composite surface morphology mapping, 5000×magnification, (b) EDX spectra of the elements present in the associated composite, and (c) EDX mapping of the three most elements composing the associated composite. Here, green, blue, and red color represents the element of oxygen (O), titanium (Ti), and carbon (C) respectively [23].

Fig. 6a shows agglomerated TiO_2 microparticles with various sizes from nano to micro-scale range (represented by blue color) have been distributed on the surface of ACB supporting material matrix (represented by red color) that also in agglomeration structure with various sizes of nano to micro-scale range. While, oxygen elements (represented by green color) might be the polyhydroxy of flavonoids, saponins, and tannins constructed the Aloe vera extract had also been properly distributed throughout the surface of the associated synthesized ACB-TiO_2 composite material. The original data of those are collected as an additional appendix of the reference [23] of this paper.

In addition, the percentage amount of the most much three elements composing the synthesized composite aforementioned can be displayed in the form of a triangle diagram as depicted in Fig. 6(c). This Fig. shows that elements constructed in the synthesized composite, i.e., C, O, and Ti elements had been distributed onto two areas marked as area *I* and area *II* with different compositions of the elements. For example, if we randomly take C = 60% in area *I*, Ti, and O each will be 20% and 20%. Similarly, if we take C = 20 % in area II, Ti and O will be 60% and 20 % respectively, and so on.

On the other hand, it was known that the surface area of the synthesized ACB-TiO_2 composite determined by BET-nitrogen gas adsorptive analysis was confirmed bigger than that of the original ACB used, which was about 296.1998 ± 2.7136 m^2/g compared to 191.4452 ± 2.4381 m^2/g. The original data of those are collected as an additional appendix of the reference [23] of this paper.

Nevertheless, the mechanism of entering TiO_2 microparticles into the pores of the ACB matrix and embedded on its surface in detail have not been investigated yet at all.

D. Photocatalytic Activity Test of the Synthesized ACB-TiO2 Composite

The photocatalytic activity of the synthesized ACB-TiO_2 composite had been tested towards methyl orange (MO) dye solution of 100 ppm concentration for about 4 hours of contacts time and the result is displayed in Fig. 7.

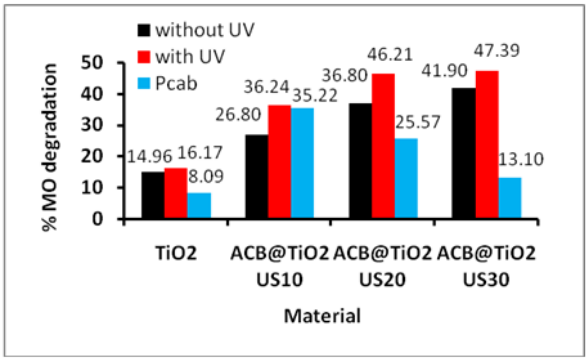

Fig. 7. Photocatalytic activity of the synthesized ACB-TiO_2 composite towards 100 ppm MO solution [23].

Fig. 7 shows the photocatalytic capability of the synthesized ACB-TiO_2 composite towards 100 ppm MO solution is significantly bigger than that of the synthesized TiO_2 microparticles originally applied, under UV light exposure as well as without UV light exposure. We can see that about 36.24%, 46.21% and 47.39% MO could be successfully photo-catalytically degraded by the ACB-TiO_2 composite synthesized through 10, 20, and 30 minutes of ultrasonic (US) agitation respectively compared to just about 16.17% MO when it was photo-catalytically degraded by the associated TiO_2 microparticles itself. The higher capability of photocatalytic activity of the synthesized ACB-TiO_2 composite compared to that of the associated TiO_2 microparticles was also well confirmed when it was applied to degrade the MO solution without UV light exposure. In this case, we can see the red color graph shown in Fig. 7, it is just about 14.96% MO has been successfully degraded by TiO_2 microparticles compared to 26.80%, 36.09%, and 41.90% MO which was successfully degraded by the ACB-TiO_2 composite synthesized through 10-, 20-, and 30-minutes US agitation respectively. These data are convincing evidence that the fabricated ACB microparticles are a useful material to significantly enhance the photocatalytic activity of TiO_2 microparticles in the form of composite materials. In this relation, the blue color graph of Fig. 7 represents the percentage increase of photocatalytic activity of TiO_2 micro-particles due to UV light exposure. We can see that it is just 8.09 % for TiO_2 compared to 35.22%, 25.57%, and 13.10%. for ACB-TiO_2 composite materials synthesized under 10, 20, and 30 minutes of US agitation respectively. This is convincing evidence that the fabricated ACB microparticles can be applied to enhance significantly TiO_2 photocatalytic activity in the form of ACB-TiO_2 composite materials.

E. Antibacterial Activity Test of the Synthesized ACB-TiO_2 Composite

The antibacterial activity of the synthesized ACB-TiO_2 composite had been tested on both gram-negative bacteria representative, *Escherichia coli (E. coli)*, and gram-positive bacteria representative, *Staphylococcus aureus (S. aureus)*, and the result is displayed in Fig. 8.

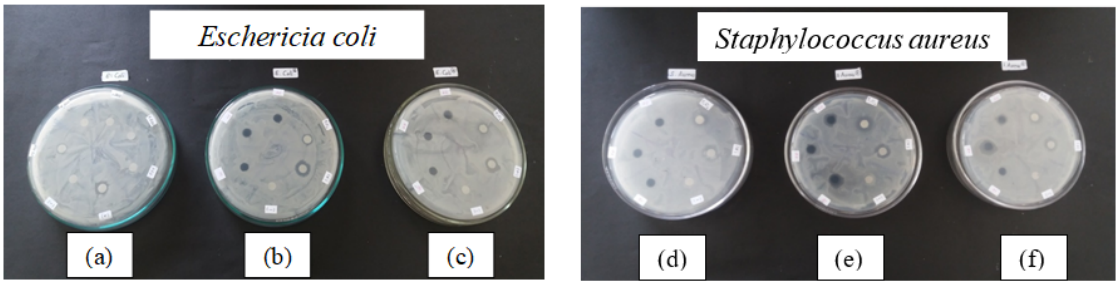

Fig. 8. The filter paper-agarose disc test result of the synthesized ACB-TiO2 composite antibacterial activity of (a) & (d) without UV light exposure, (b) & (e) 1 hour UV light exposure, (c) & (f) 2 hours UV light exposure [23].

The clear zone observable appeared around the filter paper discs that indicated the materials tested possess antibacterial activity was summarized in Table I.

Table I shows that the antibacterial activity level of the ACB-TiO_2 composite synthesized through various time US agitations of 10, 20, and 30 minutes was still lower than that of TiO_2 microparticles itself, towards *E. coli* as well as *S. aureus*. However, we can see that the antibacterial activity level of the ACB-TiO_2 composite synthesized through 30 minutes of US agitation was higher than that synthesized through 10 and 20 minutes of US agitation.

European Journal of Advanced Chemistry Research
www.ej-chem.org

TABLE I: THE SUMMARY OF THE CLEAR ZONE IN MM WIDE APPEARED AROUND THE FILTER PAPER DISCS THAT INDICATED THE ANTIBACTERIAL ACTIVITY LEVEL OF THE SYNTHESIZED ACB-TiO_2 COMPOSITE

Sample*	*E. coli* clear zone/ mm			*S. aureus* clear zone/ mm		
	Without UV light exposure	1 hour of UV light exposure	2 hours of UV light exposure	Without UV light exposure	1 hour of UV light exposure	2 hours of UV light exposure
Positive control	3.85	4.25	4.40	5.55	5.55	5.25
Negative control	0.55	0.60	0.50	0.95	1.10	0.95
US10	0.2	0.05	0.50	0.25	4.10	0.20
US20	1.25	0.70	0.55	0.50	4.20	3.75
US30	1.35	1.50	1.60	0.70	4.55	3.70
TiO_2MPs	2.00	3.10	2.40	4.20	5.45	3.90

*US10, US20, and US30 are the ACB-TiO_2 composites synthesized through 10, 20, and 30 minutes of ultrasonic agitation respectively [23].

The facts demonstrated that the duration exposure of US agitation is one of the important techniques for the synthesis of ACB-TiO_2 composite materials. In this relation, the longer the US agitation will produce the better the antibacterial activity of the synthesized ACB-TiO_2 composite materials. To investigate how long the US agitation should be exposed during the synthesis of ACB-TiO_2 composite for the best antibacterial activity can be conducted by plotting the clear zone diameter that appeared around the filter paper disc versus the duration time of US agitations applied as depicted in Fig. 9. Applying the equation of $y = 0.005x^2 - 0.145 + 1.45$ (for *E. coli*) and $y = 0.001x^2 - 0.027x + 4.25$ (for *S. aureus*) where y and x is clear zone diameter and US agitation time respectively, we can predict how long the US agitation should be exposed to synthesize the ACB-TiO_2 composite materials for the best antibacterial activity. By substituting y with the widest clear zone shown in Table I, i.e. 4.40 mm for E. coli and 5.55 mm for S. aureus into the equations of $y = 0.005x^2 - 0.145 + 1.45$ (for E. coli) and $y = 0.001x^2 - 0.027x + 4.25$ (for S. aureus) we can predict that US agitation exposed for about 43 minutes and 52 minutes on the synthesis process of ACB-TiO_2 composite would be able to enhance the TiO_2 microparticles antibacterial activity become much higher than its original, even it is possible up to the same as the antibacterial activity level of the positive control used, amoxicillin antibiotic. The facts also demonstrated that the synthesized ACB microparticles are very important and useful supporting material to fabricate ACB-TiO_2 composite with bifunctional properties, i.e., powerful photocatalytic and at once powerful antibacterial materials.

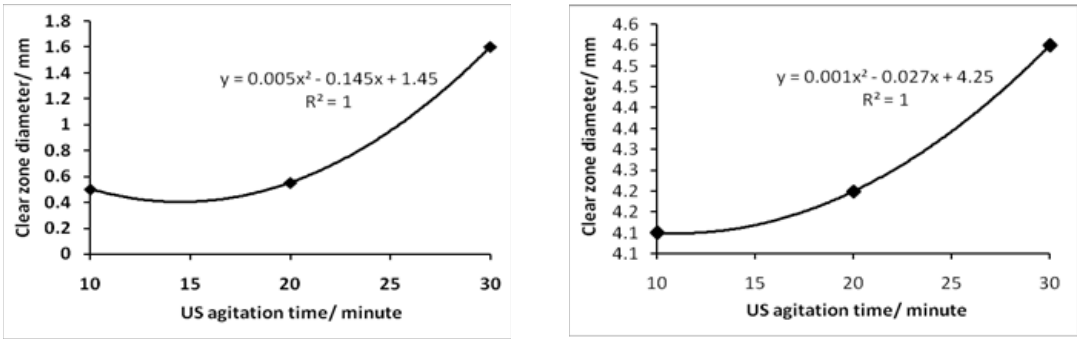

(a) (b)

Fig. 9. Plotting curve of the clear zone diameter versus US agitation time for (a) *E. coli*, and (b) *S. aureus* antibacterial activity of the synthesized ACB-TiO_2 composite materials.

IV. CONCLUSION

It can be concluded that functional ACB-TiO_2 composite materials have been successfully synthesized from activated carbon black (ACB) and TiO_2 microparticles using ultrasonic agitation of 30 minutes optimum time. The photocatalytic-antibacterial activity of the synthesized ACB-TiO_2 composite at the optimum time of ultrasonic agitation was significantly increased following the mathematical quadratic equation of $y = ax^2 + bx + c$ where y is the clear zone diameter revealed around the filter paper disc of about 1 cm in diameter, x is ultrasonic agitation time applied in the synthesis of ACB-TiO_2 composite material, and a, b, c is the quadratic equation constant of $0 < a < 1$; $-1 < b < 0$ and $c > 1$. Overall, the both photocatalytic and antibacterial activity of TiO_2 microparticles can be enhanced significantly by using ACB microparticles in the form of ACB-TiO_2 composite material. The fact already described above indicates that the composite synthesized from ACB microparticles and TiO_2 ones is very potent to be developed further for bacterial sensor materials in the next future by enhancing its electrical and optical properties employing the most suitable materials.

ACKNOWLEDGMENT

The authors are grateful to the rector of Diponegoro University, and the head of the Research and Community Service Institution of Diponegoro University for the financial support to do this research.

FUNDING

The financial support from Diponegoro University through an International Publication Research grand schema with the PNBP DIPA budgeting source of number SP DIPA–042.01.2.400898/2016, December 7, 2015, the fiscal year 2016.

CONFLICT OF INTEREST

The authors declare not any conflict of interest related to the financial support as well as personal relationship in this paper.

REFERENCES

[1] Smith WF, Hashemi J. *Foundations of Materials Science and Engineering.* (4th.Ed.). McGraw Hill International Edition Singapore; 2006.
[2] Osman AF, Alakrach AM, Kalo H, Azmi WNW, Hashim F. In vitro biostability and biocompatibility of Ethyl vinyl acetate (EVA) nanocomposites for biomedical applications. *RSC Advances* 2015; 5: 31485-31495. doi: 10.1039/C4RA15116J.
[3] Chen B, Meng Y, Sha J, Zhong C, Hu W, Zhao N. Preparation of MoS_2/TiO_2 based nanocomposites for Photocatalysis and Rechargeable batteries: Progress, Challenges, and Perspective. *Nanoscale* 2018; 10: 34-68. doi:10.1039/C7NR07366F.
[4] Jagadish K, Chandrashekar BN, Byrappa K, Rangappa KS, Srikantaswammy S. Simultaneous removal of dye and heavy metals in a single step reaction using PVA/MWCNT composite. *Anal.Methods* 2016; 8: 2408-2412. doi: 10.1039/c6ay00229c.
[5] Mammadov G, Ramazanov MA, Kanaev A, Hasanova UA, Huseynov KA. Photocatalytic degradation of organic pollutants in air by application of Titanium dioxide nanoparticles. *CET,* 2017; 60: 241-246. doi: 10.3303/CET1760041.
[6] Abdennouri M, Baalala M, Galadi A, El Makhfouk M, Bensitel M, Nohair K, Sadiq M, Boussaound A, Barka N. Photocatalytic degradation of pesticides by Titanium dioxide and Titanium pillared purified clays. *Arab. J. Chem.* 2016; 9: S313-S318. doi: 10.1016/j.arabjc.2011.04.005.
[7] Mahlambi MM, Ngila CJ, Mamba BB. Recent developments in environmental photocatalytic degradation of organic pollutants: The case of Titanium dioxide nanoparticles-A Review. *J. Nanomater.* 2015:1-30. doi: 10.1155/2015/790173.
[8] Kabra K, Chaudhary R, Sawhney RL. Treatment of hazardous organic and inorganic compounds through aqueous-phase photocatalysis: A Review. *Ind. Eng. Chem. Res*. 2004; 43(24):7683-7696. doi: 10.1021/ie0498551.
[9] Hoffmann MR, Martin ST, Choi W, Bahnemann DW. Environmental applications of semiconductor photocatalysis. *Chem. Rev.*1995; 95(1): 69-96. doi: 10.1021/cr00033a004.
[10] Atefyekta S, Ercan B, Karlsson J, Taylor E, Chung S, Webster T, Andersson M. Antimicrobial performance of mesoporous titania thin films: role of pore size, hydrophobicity, and antibiotic release. *Int. J. Med.* 2016; 11: 977-990. doi: 10.2147/IJN.S95375.
[11] Sujata SA, Jack NA. Titanium dioxide nanoparticle as an environmental sanitazing agent. *JMBT* 2015; 7(2): 061-064. doi: 10.4172/1948-5948.1000183.
[12] Petica A, Florea A, Gaidau C, Balan D, Anicai L. Synthesis and characterization of silver-titania nanocomposites prepared by electrochemical method with enhanced photocatalytic characteristics, antifungal and antimicrobial activity. *J. Mater. Res. Technol*. 2019; 8(1): 41-53. doi: 10.1016/j.jmrt.2017.09.009.
[13] Zimbone M, Buccheri MA, Cacciato G, Sanz R, Rappazzo G, Boninelli S, Reitano R, Romano L, Privitera V, Grimaldi MG. Photocatalytic and antibacterial activity of TiO_2 nanoparticles obtained by laser ablation in water. *Appl. Catal. B* 2015; 165: 487-494. doi: 10.1016/j.apcatb.2014.10.031.
[14] Kubacka A, Diez MS, Rojo D, Bergiela R, Ciordia S, Zapico I, Albar JP, Barbas C. Martin dos Santos VAP, Garcia MF, Ferrer M. Understanding the antimicrobial mechanism of TiO_2-based nanocomposite films in a pathogenic bacterium. *Sci. Rep.* 2014; 4: 4134. doi: 10.1038/srep04134.
[15] Yadav HM, Otari SV, Bohara RA, Mali SS, Pawar SH, Delekar SD. Synthesible light photocatalytic antibacterial activity of nickel-doped TiO_2 nanoparticles against Gram-positive and Gram-negative bacteria. *JPPA* 2014; 294: 130-136. doi: 10.1016/j.jphotochem.2014.07.024.
[16] Chakra CS, Rajendar V, Rao KV, Kumar M. Enhanced antimicrobial and anticancer properties of ZnO and TiO_2 nanocomposites. *3Biotech* 2017; 7 (89): doi: 10.1007/s13205-017-0731-8.
[17] Santosh SM, Kandasamy N. Antibiofilm activity of epoxy/Ag-TiO_2 polymer nanocomposite coatings against *Staphylococcus Aureus* and *Escherichia Coli. Coatings* 2015; 5:95-114. doi: 10.3390/coatings5020295.
[18] Bonilla AM, Cerrada ML, Garcia MF, Kubacka A, Ferrer M, Garcia Mc.F. Biodegradable polycaprolactone-titania nanocomposite: preparation, characterization and antimicrobial properties. *Int. J. Mol. Sci.* 2013; 14: 9249-9266. doi: 10.3390/ijms14059249.
[19] Desai V, Naik B, Ghosh NN, Kowshik M. Functionalization of AgCl/TiO_2 nanocomposite with folic acid: a promising strategy for enhancement of antimicrobial activity. *Sci. Adv. Mater*. 2013; 5(5): 431-439. doi: 10.1166/sam.2013.1472.
[20] Fu X, Clark LA, Yang Q, Anderson MA. Enhanced photocatalytic performance of Titania-based binary metal oxides: TiO_2/SiO_2 and TiO_2/ZrO_2. *Environ. Sci. Technol*. 1996; 30(2): 647-653. doi: 10.1021/es950391v.
[21] Njoku VO, Islam, MdA, Asif M, Hameed BH. Adsorption of 2,4-dichloro phenoxy acetic acid by mesoporous activated carbon prepared from H_3PO_4-activated langsat empty fruit bunch. *J. Environ. Manage.* 2015; 154(15):138-144. doi: 10.1016/j.jenvman.2015.02.002.
[22] Ganapathi RK, Ashok CH, Venkateswara RK, Shilpa C, Tambur P. Green synthesis of TiO_2 nanoparticles using Aloe vera extract. *IJARPS* 2016; 2(1A):28–34. URL: www.arcjournals.com.

[23] Mega F. Green Synthesis and Characterization of The Functional Nanocomposite of Activated Carbon-Titanium Dioxide: The study of the effect of time toward the Antibacterial Activity and Photocatalytic Properties), Undergraduate Final Project (S1 Scription), Diponegoro University 2017.
[24] López A, Tangil MSD, Orellana OV, Ramírez AS, Rico M. Phenolic constituents, antioxidant and preliminary antimycoplasmic activities of leaf skin and flowers of Aloe vera L. Burm. f. (syn. A. barbadensis Mill.) from the Canary Islands (Spain). *Molecules* 2013; 18(5): 4942–4954. doi: 10.3390/molecules18054942.
[25] Wang TH, Lópe AMN, Li S, Dixon DA. Hydrolysis of $TiCl_4$: Initial steps in the production of TiO_2. *J. Phys. Chem. A*. 2010; 114(28): 7561-7570. DOI: 10.1021/jp102010h.
[26] Mittal AK, Chisti Y, Banerjee UC. Synthesis of metallic nanoparticles using plant extracts. *Biotechnol. Adv*. 2013; 31(2):346–356. doi: 10.1016/ j.biotechadv.2013.01.003.
[27] Maurya A, Chauhan P, Mishra A, Pandey AK. Surface functionalization of TiO_2 with plant extracts and their combined antimicrobial activities against *E. faecalis* and *E. Coli*. *J. Res. Updates Polym. Sci.* 2012; 1(12):43–51. doi: 10.6000/1929-5995.2012.01.01.6.
[28] Bracamonte MV, Lacconi GI, Urreta SE, Torres LEFF. On the nature of defects in liquid-phase exfoliated graphene. *ACS J. Phys. Chem*. 2014; 1(6):1–4. doi: 10.1021/jp051930a.